Viewpoint

Rising CO$_2$ and warming reduce global canopy demand for nitrogen

Ning Dong[1,2], Ian J. Wright[2,3], Jing M. Chen[4], Xiangzhong Luo[5], Han Wang[6], Trevor F. Keenan[7,8], Nicholas G. Smith[9], Iain Colin Prentice[1,2,6]

[1]Georgina Mace Centre for the Living Planet, Imperial College London, Department of Life Sciences, Silwood Park Campus, Ascot SL5 7PY, UK

[2]Department of Biological Sciences, Macquarie University, North Ryde, NSW 2109, Australia

[3]Hawkesbury Institute for the Environment, Western Sydney University, Locked Bag 1797, Penrith, NSW 2751, Australia

[4]Department of Geography and Planning, University of Toronto, 100 George Street, Toronto, Ontario, Canada MS5 3G3

[5]Department of Geography, National University of Singapore, 1 Arts Link, Singapore 117570

[6]Department of Earth System Science, Ministry of Education Key Laboratory for Earth System Modelling, Institute for Global Change Studies, Tsinghua University, Beijing 100084, China.

[7]Department of Environmental Science, Policy and Management, UC Berkeley, Berkeley, California

[8]Climate and Ecosystem Sciences Division, Lawrence Berkeley National Laboratory, Berkeley, California

[9]Department of Biological Sciences, Texas Tech University, Lubbock, TX 79409, USA

Corresponding email: ning.dong@imperial.ac.uk, tel: 447442037409,

ND: 0000-0003-0793-8854

IJW: 0000-0001-8338-9143

JMC: 0000-0002-8682-1293

XZL: 0000-0002-9546-0960

HW: 0000-0003-2482-1818

TFK: 0000-0002-3347-0258

NGS:0000-0001-7048-4387

ICP: 0000-0002-1296-6764

Summary

Nitrogen (N) limitation has been considered as a constraint on terrestrial carbon uptake in response to rising CO_2 and climate change. By extension, it has been suggested that declining carboxylation capacity (V_{cmax}) and leaf N content in enhanced-CO_2 experiments and satellite records signify increasing N limitation of primary production. We predicted V_{cmax} using the coordination hypothesis, and estimated changes in leaf-level photosynthetic N for 1982–2016 assuming proportionality with leaf-level V_{cmax} at 25˚C. Whole-canopy photosynthetic N was derived using satellite-based leaf area index (LAI) data and an empirical extinction coefficient for V_{cmax}, and converted to annual N demand using estimated leaf turnover times. The predicted spatial pattern of V_{cmax} shares key features with an independent reconstruction from remotely-sensed leaf chlorophyll content. Predicted leaf photosynthetic N declined by 0.27 % yr^{-1}, while observed leaf (total) N declined by 0.2–0.25 % yr^{-1}. Predicted global canopy N (and N demand) declined from 1996 onwards, despite increasing LAI. Leaf-level responses to rising CO_2, and to a lesser extent temperature, may have reduced the canopy requirement for N by more than rising LAI has increased it. This finding provides an alternative explanation for declining leaf N that does not depend on increasing N limitation.

Key words: Photosynthetic capacity, coordination hypothesis, remote sensing, nitrogen demand, CO_2 fertilization, nitrogen cycle, leaf chlorophyll, acclimation

Introduction

Atmospheric CO_2 has increased from about 280 to nearly 420 μmol mol^{-1} (in 2022) since the Industrial Revolution. This increase is smaller than expected from the cumulative anthropogenic emissions of CO_2. The difference is partly due to terrestrial ecosystems, which have taken up

around one-third of these emissions (Friedlingstein *et al.*, 2021). There is concern, however, that this 'terrestrial carbon sink' may not persist due to increasing limitation of primary production by nutrient availability (Reich *et al.*, 2006). Much of this literature has focused on nitrogen (N) as a limiting nutrient, hence our focus on N here – although we recognize that other plant nutrients (notably phosphorus) may be more important in constraining primary production in the tropics, and in regions with high rates of N deposition.

The incorporation of carbon-nitrogen (C-N) cycle coupling has become a priority in the development of dynamic global vegetation models (DGVMs), partly in order to address concerns about the persistence of the terrestrial carbon sink. But there is little consensus as to how C-N coupling should be represented in DGVMs. The mechanisms by which plants acquire additional N in response to elevated CO_2 (e.g. Finzi *et al.*, 2007) are often not well represented in DGVMs (Zaehle *et al.*, 2014). Meanwhile, satellite-derived records of global changes in chlorophyll content, and independent measurements of leaf N content, have been used to quantify trends in ecosystem C-N coupling (He *et al.*, 2017; Penuelas *et al.*, 2020 and references therein). It has been found that leaf N is declining, and inferred that N limitation (i.e. an excess of N demand over supply) is increasing. Moreover, increasing N limitation has been taken to imply a reduction in the CO_2 fertilization effect on gross primary production (GPP). As this effect is considered to be a significant mechanism driving the terrestrial carbon sink (Walker *et al.*, 2021), increasing N limitation has been taken to imply a potential reduction in the efficiency of this sink (He *et al.*, 2017; Wang *et al.*, 2020) – albeit that other mechanisms, whose relative magnitudes are still uncertain, may also contribute (Walker *et al.*, 2021).

Here we interrogate the idea of increasing N limitation by considering how leaf photosynthetic N might be *expected* to change with rising CO_2 and warming, based on leaf-level optimality principles. We also consider how changes in leaf photosynthetic N might translate into changes in whole-canopy photosynthetic N (given observed increases in leaf area index, LAI) and the annual canopy demand for N (which also depends on the rate at which leaves are replaced, and the efficiency with which the N in sensescing leaves is resorbed). Studies have shown that leaf N is influenced by environmental factors during growth, including temperature and CO_2 (Ainsworth & Long, 2005; Dong *et al.*, 2017; Smith & Keenan, 2020). Many of these responses are predicted by the coordination hypothesis, which states that the Rubisco- and electron transport-limited rates of photosynthesis tend to be co-limiting under typical daytime conditions (Chen et al, 1993; Dong *et al.*, 2017). According to this hypothesis, leaf-level V_{cmax} should acclimate such that currently

available light is fully utilized. A growing body of both experimental (Scafaro *et al.*, 2017) and observational (Dong *et al.*, 2017; Smith *et al.*, 2019) evidence supports the predictions of this hypothesis with respect to both experimentally imposed changes and spatial gradients in plants' light environment, growth temperature and atmospheric dryness (vapour pressure deficit, VPD). V_{cmax} when standardized to a common temperature (typically 25˚C, written here as V_{cmax25} and taken to be proportional to Rubisco content) is predicted to increase in proportion to absorbed light; to decline with increasing growth temperature, even as V_{cmax} measured at growth temperature increases; and to increase with VPD, compensating for greater stomatal closure. V_{cmax} at growth temperature increases to counteract increased photorespiration at higher temperatures (Smith *et al.,* 2019), while V_{cmax25} declines because less Rubisco is required (Scafaro *et al.,* 2017) to achieve a given photosynthetic rate – this second effect being stronger than the first (Fig. 1).

Free Air Carbon Enrichment (FACE) experiments (Ainsworth & Long, 2005), and comparisons between plants growing in natural CO_2 springs and in control plots (Saban et al., 2018), have shown that leaf-level photosynthetic capacity (V_{cmax}) and leaf N generally decline with enhanced CO_2. This decline is predicted by the coordination hypothesis due to the different sensitivities of Rubisco- and electron transport-limited photosynthesis to CO_2. The Rubisco-limited rate is more sensitive, so – all else equal – the optimal Rubisco content of leaves should decline as CO_2 increases; otherwise, plants would have to bear the cost of maintaining Rubisco in excess of the amount they need in order to use the available light. Fig. 1 shows that the coordination hypothesis predicts the generally decreasing trend of experimentally induced reductions in V_{cmax} as growth CO_2 is increased (Zheng *et al.*, 2019). Although these data show unexplained deviations from a smooth curve, the comparison (for soybean) is apposite because photosynthesis in this N-fixing plant is unlikely to be limited by N supply. But declining V_{cmax} and leaf N with increasing CO_2 are also observed in C_3 plants more generally, and the coordination hypothesis supplies a simple and parsimonious explanation (Smith & Keenan, 2020).

In this opinion article, we have used the coordination hypothesis to predict V_{cmax}, yielding a global spatial pattern similar to that presented by Smith *et al.* (2019), and compared this predicted spatial pattern with a recently developed, remotely sensed map of leaf-level chlorophyll content (LCC). LCC has been shown to be tightly linked to V_{cmax} (Luo *et al.*, 2019, Luo *et al.*, 2021). We then predicted temporal variation in V_{cmax} at growth temperature from the beginning of the satellite era (1982–2016) using the coordination hypothesis; converted predicted V_{cmax} to V_{cmax25} using the Arrhenius equation; and converted predicted changes in V_{cmax25} to changes in leaf-level

photosynthetic (Rubisco) N. We further estimated changes in whole-canopy photosynthetic N, taking into account satellite-derived changes in LAI, with the help of an empirical extinction coefficient describing the decline in leaf-level V_{cmax} with canopy depth. Finally, we estimated how the annual leaf- and canopy-level demand for N uptake has changed over time, with the help of leaf turnover times separately estimated for different phenological types (evergreen versus deciduous plants).

Methods

LCC has been estimated using radiative transfer theory to downscale remotely sensed canopy reflectance to leaf reflectance, as input to a leaf optical model (Luo *et al.*, 2019). Croft *et al.* (2020) thereby retrieved global monthly LCC from land-surface spectral reflectance data provided by the Medium Resolution Imaging Spectrometer (MERIS) instrument aboard Envisat. MERIS provided red, near-infrared, and red-edge bands at 300 m spatial resolution for seven-day intervals during 2003 to 2012. The correlation between chlorophyll and V_{cmax} was used to map global V_{cmax} based on LCC, using empirical relationships between V_{cmax25} and LCC for different plant functional types (Luo *et al.*, 2019). However, whereas Luo *et al.* (2019) labelled their mapped quantity as V_{cmax25}, our analysis presupposes that LCC is more closely related to V_{cmax} at growing-season temperature than to V_{cmax25}. The empirical relationships used to relate V_{cmax} and LCC were based on measurements made in a narrow range (17–20˚C) before adjustment to 25˚C (Teklemariam *et al.*, 2009), so relationships of V_{cmax} or V_{cmax25} to LCC could not be distinguished in those measurements.

Optimal V_{cmax} values according to the coordination hypothesis were estimated using the following expression (Dong *et al.*, 2017) for C_3 plants acclimated to their growth conditions:

$$V_{cmax} \approx \varphi_0 I_0 (c_i + K)/(c_i + 2\Gamma^*) \tag{1}$$

where φ_0 is the intrinsic quantum efficiency of photosynthesis (mol mol^{-1}), I_0 is the incident photosynthetic photon flux density (PPFD) (µmol m^{-2} s^{-1}), c_i is the intercellular partial pressure of CO_2 (Pa) (for simplicity, and in line with most of the current plant functional ecology and carbon-cycle modelling literature, we have disregarded the limitation imposed by finite mesophyll conductance), K is the effective Michaelis-Menten coefficient of Rubsico (Pa), and Γ^* is the photorespiratory compensation point (Pa). Equation (1) is a generic expression, independent of the

precise formulation of J_{max} limitation effects (models used by Wang *et al.*, 2017 and Smith *et al.*, 2019, for example, used slightly differing empirical formulations of the response of electron transport to light). Reference values and temperature dependencies of φ_0, K and Γ^* in equation (1) were derived from Bernacchi *et al.* (2001). Values of c_i in equation (1) were estimated by the least-cost hypothesis as described in Prentice *et al.* (2014):

$$c_i = \Gamma^* + (c_a - \Gamma^*) \, \xi / (\xi + \sqrt{D_0}), \text{ where} \tag{2a}$$

$$\xi = \sqrt{[\beta (K + \Gamma^*)/1.6 \, \eta^*]}. \tag{2b}$$

Equation (2) yields the c_i value (for a given ambient CO_2 partial pressure, c_a) that minimizes the sum of the costs (per unit assimilation) of maintaining the capacities for transpiration and carboxylation. The parameter ξ (Pa$^{\frac{1}{2}}$) is inversely related to the sensitivity of stomata to VPD (D_0). The scaling factor β was estimated as 146 from a global analysis of leaf $\delta^{13}C$ measurements (Wang *et al.,* 2017). η^* is the viscosity of water at growth temperature, relative to its value at 25°C. V_{cmax} was converted to V_{cmax25} by inverse application of the Arrhenius equation with activation energy as given in Bernacchi *et al.* (2001).

Rubisco is the most abundant photosynthetic protein in the leaf. Photosynthetic proteins together account for 50–60% of leaf N, and Rubisco alone 25–30%. We used the N in Rubisco as an index of total photosynthetic N (Evans and Seemann, 1989), implicitly assuming that other proteins – including those involved in electron transport as well as the Calvin cycle – covary in proportion with Rubisco. The leaf N required for Rubisco ($N_{rubiscoL}$, g m^{-2} leaf area) was estimated from V_{cmax25} as follows (Dong *et al.*, 2017):

$$N_{rubiscoL} = V_{cmax25} \, M_n \, M_r \, [N_r] / (n \, k_{cat}) \tag{3}$$

where $M_n = 14$ g mol^{-1} is the molecular mass of N; $M_r = 0.55$ g μmol^{-1} is the molecular mass of Rubisco; $[N_r] = 0.0114$ mol g^{-1} is the nitrogen concentration of Rubisco; $n = 8$ is the number of catalytic sites per mole of Rubisco; and $k_{cat} = 3.5$ s^{-1} is the catalytic turnover number at 25˚C. To scale up leaf Rubisco N to the canopy, we used a big-leaf approximation:

$$N_{rubiscoC} = (1 - e^{-kL}) \, N_{rubiscoL}/k \tag{4}$$

where $N_{rubiscoC}$ (g m^{-2} ground area) is the canopy Rubisco N; L is the LAI; and k is the extinction coefficient for V_{cmax}, assigned the value of 0.175 based on its median value in studies summarized

by Lloyd *et al.* (2010). Equation (4) accounts for the declining leaf-level V_{cmax} and Rubisco N with depth in the canopy, and results in a non-linear response of Rubisco N to L. In our main analysis, L was estimated from monthly Moderate Resolution Imaging Spectroradiometer (MODIS) normalized difference vegetation index (NDVI) LAI3g from 1982–2016. There are substantial differences in temporal variations among satellite-based LAI products (Jiang *et al.*, 2017). We therefore also tried other LAI products: TCDR LAI during 1982–2016; GLASS LAI during 1982–2014; and GLOBMAP LAI during 1982–2011 (Jiang *et al.*, 2017). Differences among products are especially apparent before 2000, the first year after the launch of the Terra satellite (Fig. S1), and significant differences persist (Jiang *et al.*, 2017; Cortés *et al.*, 2021). However, with continuous improvement, most LAI products have become consistent in showing long-term positive trends in many regions (Chen *et al.*, 2019; Cortés *et al.*, 2021).

We estimated the annual leaf-level demand for photosynthetic N by:

$$N_{demandL} = (1 - c) N_{rubiscoL} / \tau \tag{5}$$

(with a parallel expression for the canopy level relating $N_{demandC}$ to $N_{rubiscoC}$) where c is the N resorption efficiency, set at 0.5 for woody vegetation and zero for herbaceous vegetation (Aerts, 1996), and τ is the leaf replacement time (years). For deciduous vegetation, τ was set to 1 year. For evergreen vegetation, $\tau = \tau_{ev}$ was estimated from the theoretical framework developed by Wang *et al.* (2021) for the leaf economics spectrum (Wright et al., 2004), which relates leaf mass-per-area (LMA, g m^{-2}) to leaf lifespan:

$$\tau_{ev} = \text{LMA} \, x \, (2 \, u \, C / f)^{1/2} / k \, \Sigma I_0 \tag{6a}$$

where

$$x = [h_T^{1/2} / \varphi_0] \, (c_i + 2 \, \Gamma^*) / [(c_i - \Gamma^*) \, (c_i + K)]^{1/2} \tag{6b}$$

Here $u = 768$ (dimensionless) is a constant that relates the leaf ageing rate to LMA and photosynthetic capacity, and $C = 23$ (dimensionless) is a multiplier that accounts for the total costs of constructing leaves and other tissues required to support them. Both parameters were estimated from data by Wang *et al.* (2021). f is the growing-season length, as a fraction of the year; $k = 30$ g (dry biomass) mol^{-1} (C) is a conversion factor between carbon and dry biomass; ΣI_0 is the daily total average photosynthetic photon flux density (PPFD) (mol m^{-2} day^{-1}); and h_T is the Arrhenius

function for the response of V_{cmax} to temperature, relative to its value at 25°C (Wang *et al.*, 2021). LMA for evergreen plants was derived from a scaled-up global trait data set (Fig. S2c). Herbaceous vegetation was treated as deciduous in climates with at least one month's mean temperature < 0°C, otherwise as evergreen. This is a rough approximation that accounts for the fact that herbaceous biomass commonly turns over annually in cold-winter climates. It is unrealistic for semi-arid vegetation, but we assume the consequences are minor for global totals. Evergreen, deciduous and herbaceous vegetation fractions were assigned based on ESA CCI land cover products at 0.5° resolution (Li *et al.*, 2018). The thermal growing season was defined as the period with daily mean temperatures (linearly interpolated between months) > 0°C. Fig. S2 shows values of τ and LMA used in these calculations.

Mean values of air temperature (T, °C), VPD (D_0, Pa) and total (ΣI_0, mol m^{-2} day^{-1}) and average (I_0, μmol m^{-2} s^{-1}) PPFD during the thermal growing season were calculated based on the CRU TS4.3 climate data for 1982–2016 at 0.5° resolution. Mean daytime air temperature was estimated from daily temperature maxima and minima by sinusoidal interpolation. Three historical simulations were performed: (1) all factors (CO_2, climate) varied; (2) climate varied, with CO_2 fixed at 340 ppm (its value in 1982); (3) CO_2 varied, with climate variables fixed at their mean values from 1982 to 2016. Theil-Sen regression slopes were fitted to indicate the direction and magnitude of the trends. The Theil-Sen regression slope is the median slope of all straight lines joining pairs of data points, and provides a robust estimate that is less sensitive to outliers than ordinary least-squares linear regression. Theil-Sen regression was implemented using the '*spatialEco*' package in R. Segmented regressions ('*segmented*' package) were applied to assess the timing of breaks in the time series of predicted canopy-level N demand based on each of the LAI data products. We also mapped the spatial pattern of the historical simulation based on CO_2, climate and LAI. All analyses and graphics were developed in R.

Results

The global pattern of predicted V_{cmax} at growing-season temperature (Fig. 2a) shows good general agreement with satellite LCC-derived V_{cmax} (Fig. 2b) ($r = 0.56$, p < 0.001). There is underestimation in predominantly cropland areas in interior North America, Europe and East Asia. The LCC-derived V_{cmax} for croplands depends on a cropland-specific conversion factor between LCC to V_{cmax}; our model did not distinguish crops from other plants, and therefore might underestimate V_{cmax} in croplands (which can be influenced by fertilization and irrigation, as well

as varietal selection). The spatial correlation increased to $r = 0.63$ after excluding croplands. There are a number of specific differences between the predicted and observed maps that we do not explore here. However, there are notable, large-scale geographic features in common, including a belt of exceptionally high values in the Sahel (consistent with recent measurements by Sibret *et al.*, 2021), high values in north-western India, and steep declines north of 50˚N. All of these features were already shown in the global map of predicted optimal V_{cmax} presented by Smith *et al.* (2019). Fig. 2 demonstrates that they are present in nature, and observable from space.

During the period from 1982 to 2016, CO_2 increased by 58.5 ppm and global mean land temperature by 0.5˚C. Predicted V_{cmax} at growing-season temperature generally increased, while V_{cmax25} decreased, in response to climate change (Fig. 3c, d). These responses are consistent with experimentally observed leaf-level responses to increasing temperature (Scafaro *et al.*, 2017). Both quantities declined in response to rising CO_2 (Fig. 3e, f). The net effect of warming and CO_2 increase was variable in sign for V_{cmax} at growing-season temperature, but showed an almost consistently negative trend for V_{cmax25} (Fig. 3a, b). The rate of decline in leaf-level photosynthetic N over the period studied was approximately 0.27 % yr^{-1}(Fig. 4a). For comparison, measured rates of decline in total leaf N have been in the range from 0.2 to 0.25 % yr^{-1} (Craine *et al.*, 2018; Penuelas *et al.*, 2020; Wang *et al.*, 2020).

Predicted leaf-level photosynthetic N was lowest in the tropics and highest at high latitudes and elevations (Fig. 5a). This first-order pattern is predicted by the coordination hypothesis as a consequence of enzyme kinetics. As temperature increases, less Rubisco is required to match the light-limited rate of photosynthesis. This gradient was partially offset by long leaf turnover times (Fig. S2b) in boreal evergreen forests, leading to a more even spatial distribution of the annual leaf-level requirement for photosynthetic N (Fig. 5c). Estimated whole-canopy photosynthetic N (Fig. 5b) was highest in forests, especially in the boreal zone. Similar to the pattern of leaf-level N, this was offset by long leaf turnover times, but canopy-level demand for photosynthetic N was nonetheless greatest in high latitudes (Fig. 5d).

Predicted trends with increasing CO_2 in both leaf-level photosynthetic N and N demand (Fig. 4a, c) were negative. At the canopy level, warming and (especially) increasing CO_2 imply decreasing demand, while LAI increases imply increasing demand (Fig. 4b, d). Since the late 1990s, however, the modelled global trend in total canopy N (in CO_2-only simulations and all-factor simulations) has been negative, despite widespread increases in LAI. Simulations based on alternative vegetation cover data sets showed greater variations, and differences from one another,

in the early part of the record (Fig. S1). However from 1997, which was the estimated breakpoint in the LAI3g time series, all-factor simulations using the four data sets consistently showed declining trends in whole-canopy photosynthetic N demand, with $p < 0.01$ for the all data sets except GLASS ($p = 0.2$) (Fig. S3).

Discussion

Despite many approximations, the general findings of our analysis are clear. Leaf photosynthetic N is *expected* to decline as CO_2 and temperatures rise, on optimality grounds, and the magnitude of this effect is compatible with observed declines in total leaf N. The comparison is not exact because our calculations refer only to the photosynthetic component of leaf N. However, the magnitude is similar. Moreover, the effect was large enough to counteract the potential increase in canopy N demand implied by observed, increasing trends in LAI.

It follows that declining leaf N does not necessarily imply increasing N limitation of primary production. In other words, declining leaf N is the predicted outcome of an acclimation process, by which plants avoid incurring maintenance costs in excess of requirements set by their growth conditions.

The terrestrial carbon sink does not solely depend on rising GPP. Terrestrial carbon uptake may be limited by factors other than N, especially in the tropics and in regions subject to anthropogenic N deposition, and influenced by changes in the residence time of carbon in ecosystems. We are not arguing for the absence of constraints on the carbon sink, today or in the future. Our analysis nonetheless suggests that declining leaf N should not, of itself, be taken to imply that N limitation of GPP has increased.

Rising CO_2 and temperatures affect land ecosystems in multiple ways. Establishing the dominant processes is a challenge. This applies particularly to N-cycle processes, because rates of N input (Wieder *et al.*, 2015), turnover and loss via different pathways (Fang *et al.*, 2015; Meyerholt *et al.*, 2020) are all challenging to determine. Moreover the biotic and environmental controls on more readily observable quantities, including leaf N, stable isotope ratios ($\delta^{15}N$) and nitrous oxide (N_2O) emissions, are incompletely understood. Global environmental changes induce competing effects, including increased N mineralization due to warming and increased N demand due to greening. Greening has been variously attributed (depending on the region) to rising CO_2, lengthening growing seasons, and land-use change (Zhu *et al.*, 2016). In addition to these opposing forces, our results suggest that the increase in N demand due to greening has been

outweighed in recent decades by a reduction in N demand due to the down-regulation of leaf-level photosynthetic N in response to rising CO_2 and warming.

Several studies have shown regional or global declines in plant nitrogen isotope signatures ($\delta^{15}N$) over recent decades (McLauchlan et al., 2017; Craine et al., 2018). These too have been attributed to increasing N limitation of plant growth (Caldararu *et al.,* 2022). However, plant $\delta^{15}N$ is not an unambiguous indicator of N limitation. Soil (and therefore plant) $\delta^{15}N$ values are influenced by the partitioning of ecosystem N losses between gaseous (N_2, N_2O, NO, NH_3) emissions and leaching (Houlton & Bai, 2009). Effects of elevated CO_2 on gaseous N emissions can be positive or negative, with increases in wetter environments and decreases in drier environments (Phillips et al., 2001). This pattern appears consistent with one shown by McLauchlan et al. (2017): warmer and drier forested regions of the USA showed increasing $\delta^{15}N$, in contrast with cooler and wetter regions.

Thus, although declining leaf N has been interpreted as an indicator of increasing N limitation on plant growth (He *et al.,* 2017), this attribution neglects the role of acclimation processes that are predicted to reduce canopy demand for N. Our calculations here indicate that these processes are of comparable magnitude to observed trends in leaf and canopy N, and large enough to counteract the increase in demand caused by increases in LAI.

Data Availability Statement

The data are published and available at https://doi.org/10.5281/zenodo.5917527

Author contributions

ND and ICP designed the study, ND carried out the data analysis and graphic, and ND, ICP, IJW interpreted the analysis, JMC, XZL and TFK provided the data, HW provided help on new LES model, NGS provided codes. ND drafted first version with the significant input from ICP, all authors contributed to the sequent manuscripts.

Supporting information

Fig S1 Time series of modelled global leaf-level $N_{rubisco}$, canopy-level $N_{rubisco}$, annual leaf-level $N_{rubisco}$ demand and annual canopy-level $N_{rubisco}$ demand with four different LAI datasets.

Fig S2 Maps of vegetation turnover rate (yr^{-1}), evergreen longevity (yr) and leaf mass per area (g m^{-2}).

Fig S3 Bivariate plots of annual canopy-level $N_{rubisco}$ demand against CO_2 after 1996, based on different LAI datasets.

References:

Aerts R. 1996. Nutrient Resorption from Senescing Leaves of Perennials: Are there General Patterns? *Journal of Ecology* **84**(4): 597-608.

Ainsworth EA, Long SP. 2005. What have we learned from 15 years of free-air CO_2 enrichment (FACE)? A meta-analytic review of the responses of photosynthesis, canopy properties and plant production to rising CO_2. *New Phytologist* **165**(2): 351-372.

Bernacchi CJ, Singsaas EL, Pimentel C, Portis Jr AR, Long SP. 2001. Improved temperature response functions for models of Rubisco-limited photosynthesis. *Plant, Cell & Environment* **24**(2): 253-259.

Caldararu S, Thum T, Yu L, Kern M, Nair R, Zaehle S. 2022. Long-term ecosystem nitrogen limitation from foliar δ15N data and a land surface model. *Global Change Biology* **28**(2): 493-508.

Chen JM, Ju W, Ciais P, Viovy N, Liu R, Liu Y, Lu X. 2019. Vegetation structural change since 1981 significantly enhanced the terrestrial carbon sink. *Nature Communications* **10**(1): 4259.

Chen JL, Reynolds JF, Harley PC, Tenhunen JD. 1993. Coordination theory of leaf nitrogen distribution in a canopy. *Oecologia* **93**(1): 63-69.

Cortés J, Mahecha MD, Reichstein M, Myneni RB, Chen C, Brenning A. 2021. Where are global vegetation greening and browning trends significant? *Geophysical Research Letters* **48**: e2020GL091496.

Craine JM, Elmore AJ, Wang L, Aranibar J, Bauters M, Boeckx P, Crowley BE, Dawes MA, Delzon S, Fajardo A, et al. 2018. Isotopic evidence for oligotrophication of terrestrial ecosystems. *Nature Ecology & Evolution* **2**(11): 1735-1744.

Croft H, Chen JM, Wang R, Mo G, Luo S, Luo X, He L, Gonsamo A, Arabian J, Zhang Y, et al. 2020. The global distribution of leaf chlorophyll content. *Remote Sensing of Environment* **236**: 111479.

Dong N, Prentice IC, Evans BJ, Caddy-Retalic S, Lowe AJ, Wright IJ. 2017. Leaf nitrogen from first principles: field evidence for adaptive variation with climate. *Biogeosciences* **14**(2): 481-495.

Evans JR, Seemann JR. 1989. The allocation of protein nitrogen in the photosynthetic apparatus: costs, consequences, and control. *Plant Biology* **8**: 183-205.

Fang Y, Koba K, Makabe A, Takahashi C, Zhu W, Hayashi T, Hokari AA, Urakawa R, Bai E, Houlton BZ, et al. 2015. Microbial denitrification dominates nitrate losses from forest ecosystems. *Proceedings of the National Academy of Sciences* **112**(5): 1470-1474.

Finzi AC, Norby RJ, Calfapietra C, Gallet-Budynek A, Gielen B, Holmes WE, Hoosbeek MR, Iversen CM, Jackson RB, Kubiske ME, et al. 2007. Increases in nitrogen uptake rather than nitrogen-use efficiency support higher rates of temperate forest productivity under elevated CO_2. *Proceedings of the National Academy of Sciences* **104**(35): 14014-14019.

Friedlingstein P, Jones MW, O'Sullivan M, Andrew RM, Bakker DCE, Hauck J, Le Quéré C, Peters GP, Peters W, Pongratz J, Sitch S, et al. 2021. Global Carbon Budget 2021. *Earth Syst. Sci. Data Discuss.* https://doi.org/10.5194/essd-2021-386.

He L, Chen JM, Croft H, Gonsamo A, Luo X, Liu J, Zheng T, Liu R, Liu Y. 2017. Nitrogen Availability Dampens the Positive Impacts of CO_2 Fertilization on Terrestrial Ecosystem Carbon and Water Cycles. *Geophysical Research Letters* **44**(22): 11,590-511,600.

Houlton BZ, Bai E. 2009. Imprint of denitrifying bacteria on the global terrestrial biosphere. *Proceedings of the National Academy of Sciences* **106**(51): 21713-21716.

Jiang C, Ryu Y, Fang H, Myneni R, Claverie M, Zhu Z. 2017. Inconsistencies of interannual variability and trends in long-term satellite leaf area index products. *Global Change Biology* **23**(10): 4133-4146.

Li W, MacBean N, Ciais P, Defourny P, Lamarche C, Bontemps S, Houghton RA, Peng S. 2018. Gross and net land cover changes in the main plant functional types derived from the annual ESA CCI land cover maps (1992–2015). *Earth Syst. Sci. Data* **10**(1): 219-234.

Lloyd J, Patiño S, Paiva RQ, Nardoto GB, Quesada CA, Santos AJB, Baker TR, Brand WA, Hilke I, Gielmann H, et al. 2010. Optimisation of photosynthetic carbon gain and within-canopy gradients of associated foliar traits for Amazon forest trees. *Biogeosciences* **7**(6): 1833-1859.

Luo X, Croft H, Chen JM, He L, Keenan TF. 2019. Improved estimates of global terrestrial photosynthesis using information on leaf chlorophyll content. *Global Change Biology* **25**(7): 2499-2514.

Luo X, Keenan TF, Chen JM, Croft H, Prentice IC, Smith NG, Walker AP, Wang H, Wang R, Xu C, et al. 2021. Global variation in the fraction of leaf nitrogen allocated to photosynthesis. *Nature Communications* **12**(1): 4866.

McLauchlan KK, Gerhart LM, Battles JJ, Craine JM, Elmore AJ, Higuera PE, Mack MC, McNeil BE, Nelson DM, Pederson N, et al. 2017. Centennial-scale reductions in nitrogen availability in temperate forests of the United States. *Scientific Reports* **7**(1): 7856.

Meyerholt J, Sickel K, Zaehle S. 2020. Ensemble projections elucidate effects of uncertainty in terrestrial nitrogen limitation on future carbon uptake. *Global Change Biology* **26**(7): 3978-3996.

Penuelas J, Fernández-Martínez M, Vallicrosa H, Maspons J, Zuccarini P, Carnicer J, Sanders TGM, Krüger I, Obersteiner M, Janssens IA, et al. 2020. Increasing atmospheric CO_2 concentrations correlate with declining nutritional status of European forests. *Communications Biology* **3**(1): 125.

Phillips RL, Whalen SC, Schlesinger WH. 2001. Influence of atmospheric CO_2 enrichment on nitrous oxide flux in a temperate forest ecosystem. *Global Biogeochemical Cycles* **15**(3): 741-752.

Prentice IC, Dong N, Gleason SM, Maire V, Wright IJ. 2014. Balancing the costs of carbon gain and water transport: testing a new theoretical framework for plant functional ecology. *Ecology Letters* **17**(1): 82-91.

Reich PB, Hungate BA, Luo Y. 2006. Carbon-Nitrogen Interactions in Terrestrial Ecosystems in Response to Rising Atmospheric Carbon Dioxide. *Annual Review of Ecology, Evolution, and Systematics* **37**(1): 611-636.

Scafaro AP, Xiang S, Long BM, Bahar NHA, Weerasinghe LK, Creek D, Evans JR, Reich PB, Atkin OK. 2017. Strong thermal acclimation of photosynthesis in tropical and temperate wet-forest tree species: the importance of altered Rubisco content. *Global Change Biology* **23**(7): 2783-2800.

Saban JM, Chapman MA, Taylor G. 2019. FACE facts hold for multiple generations; Evidence from natural CO2 springs. *Global Change Biology* **25**(1): 1-11.

Sibret T, Verbruggen W, Peaucelle M, Verryckt LT, Bauters M, Combe M, Boeckx P, Verbeeck H. 2021. High photosynthetic capacity of Sahelian C3 and C4 plants. *Photosynthesis Research* **147**(2): 161-175.

Smith NG, Keenan TF, Prentice IC, Wang H, Wright IJ, Niinemets Ü, Crous KY, Domingues TF, Guerrieri R, Yoko Ishida F, et al. 2019. Global photosynthetic capacity is optimized to the environment. *Ecology Letters* **22**(3): 506-517.

Smith NG, Keenan TF. 2020. Mechanisms underlying leaf photosynthetic acclimation to warming and elevated CO2 as inferred from least-cost optimality theory. *Global Change Biology* **26**(9): 5202-5216.

Teklemariam T, Staebler RM, Barr AG. 2009. Eight years of carbon dioxide exchange above a mixed forest at Borden, Ontario. *Agricultural and Forest Meteorology* **149**(11): 2040-2053.

Walker AP, De Kauwe MG, Bastos A, Belmecheri S, Georgiou K, Keeling RF, McMahon SM, Medlyn BE, Moore DJP, Norby RJ, et al. 2021. Integrating the evidence for a terrestrial carbon sink caused by increasing atmospheric CO2. *New Phytologist* **229**(5): 2413-2445.

Wang H, Prentice IC, Wright IJ, Qiao S, Xu X, Kikuzawa K, Stenseth NC. 2021. Leaf economics explained by optimality principles. *bioRxiv*: 430028.

Wang H, Prentice IC, Keenan TF, Davis TW, Wright IJ, Cornwell WK, Evans BJ, Peng C. 2017. Towards a universal model for carbon dioxide uptake by plants. *Nature Plants* **3**(9): 734-741.

Wang S, Zhang Y, Ju W, Chen JM, Ciais P, Cescatti A, Sardans J, Janssens IA, Wu M, Berry JA, et al. 2020. Recent global decline of CO_2 fertilization effects on vegetation photosynthesis. *Science* **370**(6522): 1295-1300.

Wieder WR, Cleveland CC, Smith WK, Todd-Brown K. 2015. Future productivity and carbon storage limited by terrestrial nutrient availability. *Nature Geoscience* **8**(6): 441-444.

Zaehle S, Medlyn BE, De Kauwe MG, Walker AP, Dietze MC, Hickler T, Luo Y, Wang Y-P, El-Masri B, Thornton P, et al. 2014. Evaluation of 11 terrestrial carbon-nitrogen cycles against observations from two temperate Free-Air CO_2 Enrichment studies. *New Phytologist* **203**: 803-822.

Zheng Y, Li F, Hao L, Yu J, Guo L, Zhou H, Ma C, Zhang X, Xu M. 2019. Elevated CO_2 concentration induces photosynthetic down-regulation with changes in leaf structure, non-structural carbohydrates and nitrogen content of soybean. *BMC Plant Biology* **19**(1): 255.

Zhu Z, Piao S, Myneni RB, Huang M, Zeng Z, Canadell JG, Ciais P, Sitch S, Friedlingstein P, Arneth A, et al. 2016. Greening of the Earth and its drivers. *Nature Climate Change* **6**(8): 791-795.
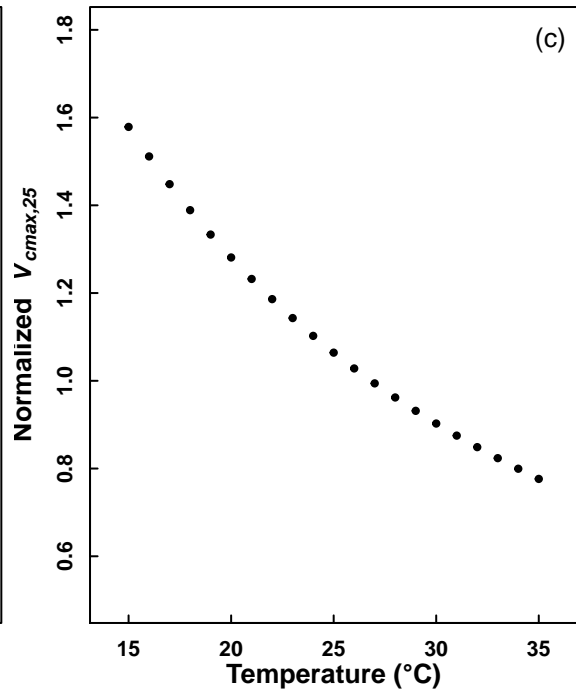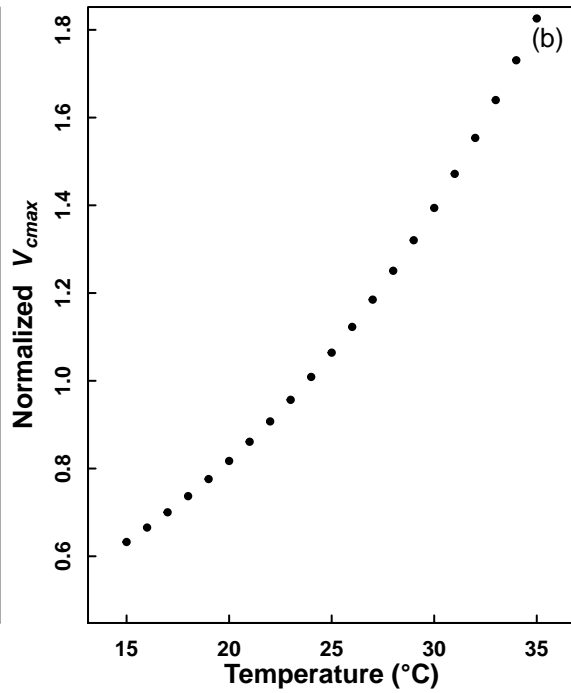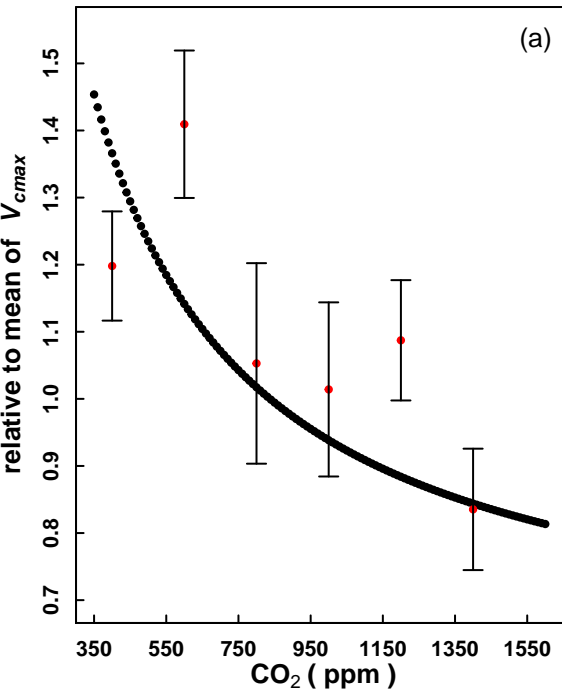
Figure legends

Fig 1 (a) The ratio of V_{cmax} (µmol m^{-2} s^{-1}) to the mean V_{cmax} over a range of growth CO_2 levels. Red dots and bars: experimental data on soybean (Zhang *et al*, 2019), showing means and 95% confidence intervals ($n = 5$ for each treatment). Black dots: predicted optimal V_{cmax} at growth temperature 25°C, photosynthetic photon flux density (PPFD) 1000 µmol m^{-2} s^{-1} and vapour pressure deficit (VPD) 1.5 kPa. (b) Predicted variations of V_{cmax} and (c) V_{cmax25} with 400 ppm CO_2 and PPFD and VPD as in (a), as a function of growth temperature. Both quantities are shown as ratios to their values at 25°C.

Fig 2. Global distributions of (a) satellite-derived V_{cmax} ($V_{cmax,chl,}$ µmol m^{-2} s^{-1}) from leaf chlorophyll content and (b) predicted V_{cmax} at growth temperature during the period from 2003 to 2012.

Fig 3 Global temporal trends (Theil-Sen slope coefficients) in predicted ($V_{cmax,}$ µmol m^{-2} s^{-1}) at growing-season temperature (left panel) and at standard temperature, 25°C ($V_{cmax25,}$ µmol m^{-2} s^{-1}) during 1982–2016 for three scenarios: (a, b) all factors; (c, d) varying climate only, with CO_2 fixed at 340 ppm; (e, f) varying CO_2 only, with climate fixed at multi-year mean values. During this period, mean annual temperatures on land increased by 0.5 °C.

Fig 4 Time series of modelled global (a) leaf-level $N_{rubisco}$ (g m^{-2} leaf area), declining by 0.27% yr^{-1} after 1996; (b) canopy-level $N_{rubisco}$ (g m^{-2} ground area), declining by 0.36% yr^{-1} after 1996; (c) annual leaf-level $N_{rubisco}$ demand (g m^{-2} leaf area year^{-1}), declining by 0.28% yr^{-1}; (d) annual canopy-level $N_{rubisco}$ demand (g m^{-2} ground area year^{-1}), declining by 0.35% yr^{-1} after 1996. Leaf area index variations were based on the LAI3g data set. Black lines: all factors varied. Blue lines: varying climate only, with CO_2 fixed at 340 ppm. Red lines: varying CO_2 only, with climate variables fixed at their multi-year mean values. The vertical grey lines in (b) and (d) indicate the breakpoint (1996) identified by segmented regression.
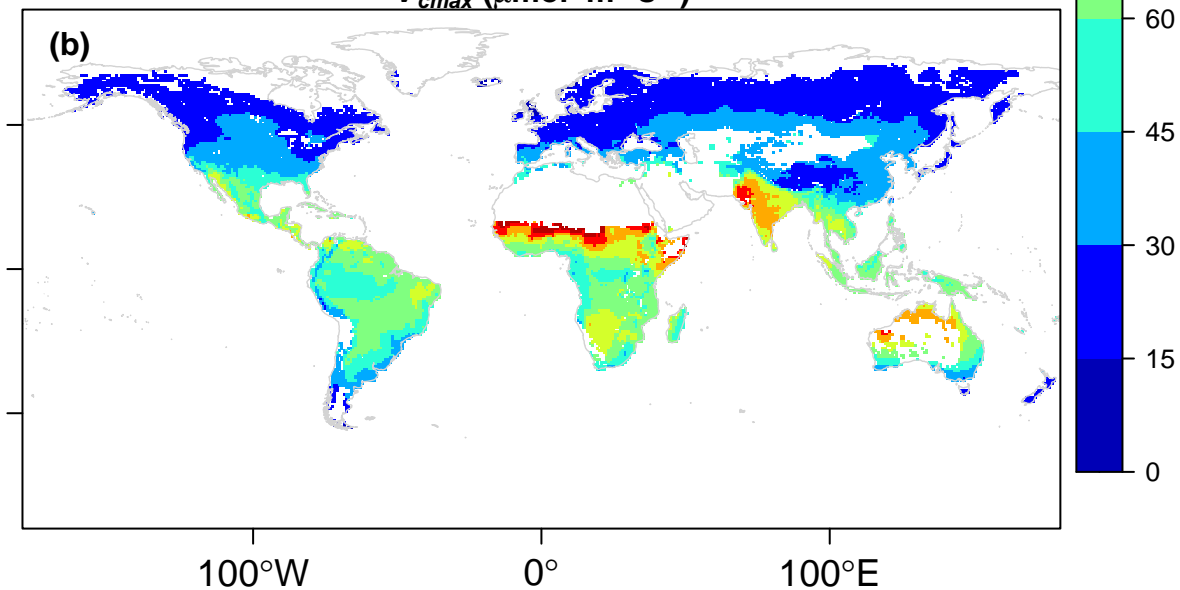
Fig 5 Predicted average global distributions of (a) leaf-level $N_{rubisco}$ (g m^{-2} leaf area), (b) canopy-level $N_{rubisco}$ (g m^{-2} ground area), (c) annual leaf-level $N_{rubisco}$ demand (g m^{-2} leaf area year^{-1}), (d) annual canopy-level of $N_{rubisco}$ demand (g m^{-2} ground area year^{-1}) over the period from 1982 to 2016. The colour scale for all map is in square root transformation.
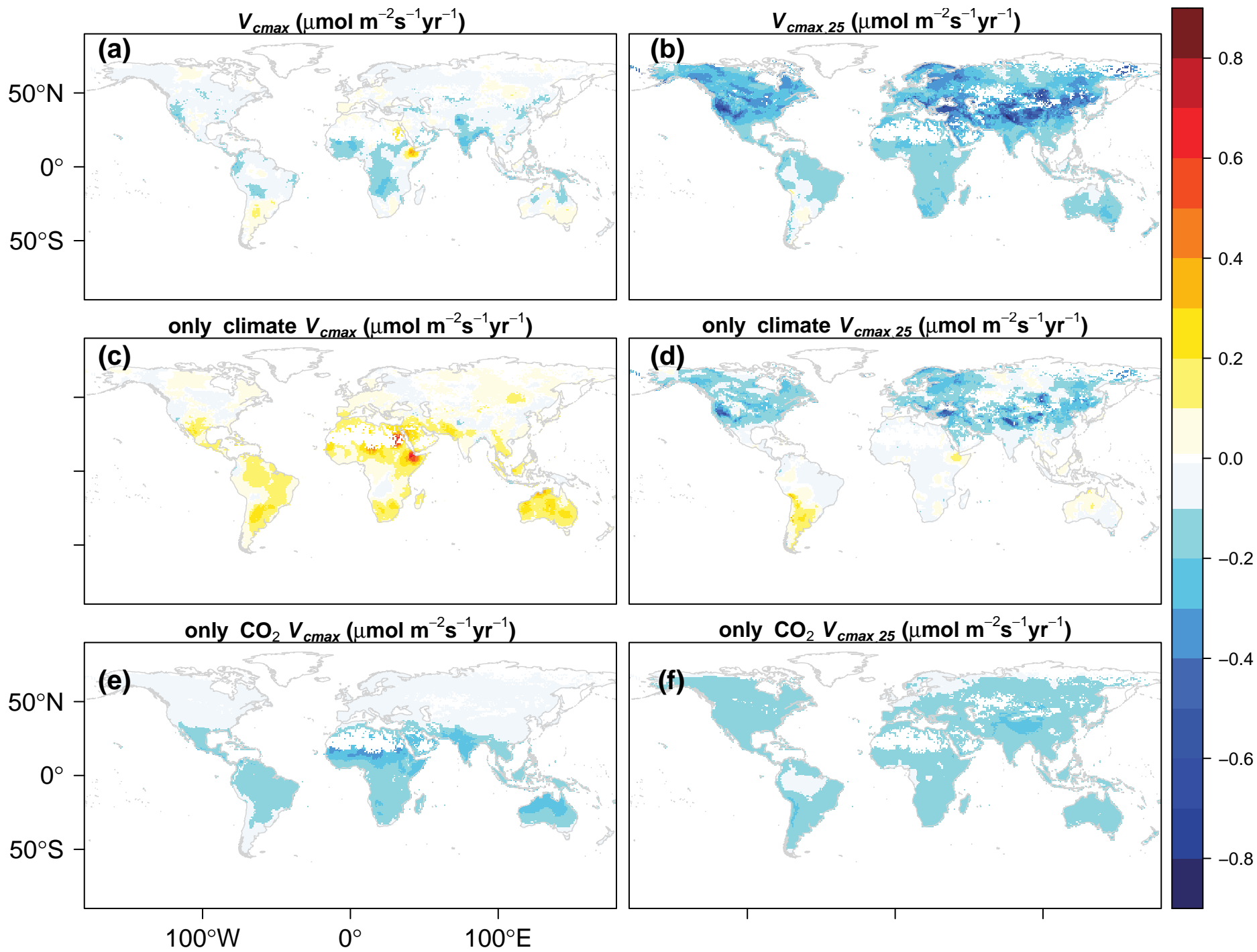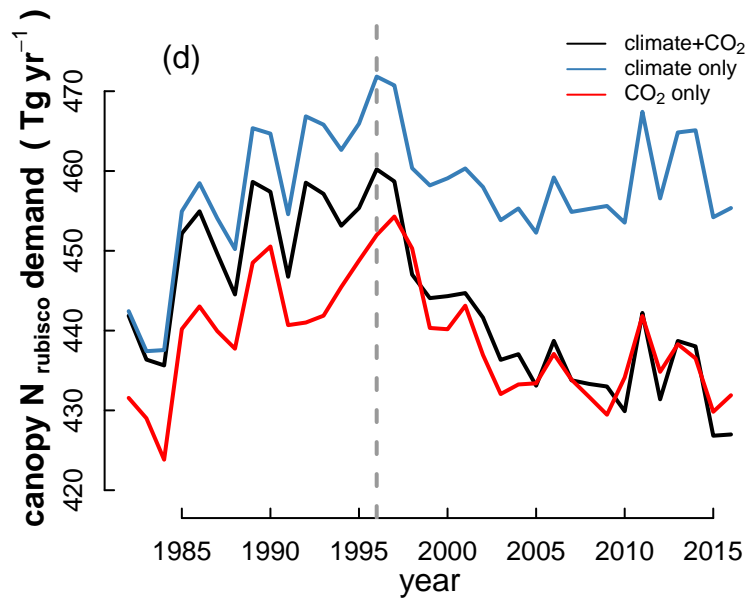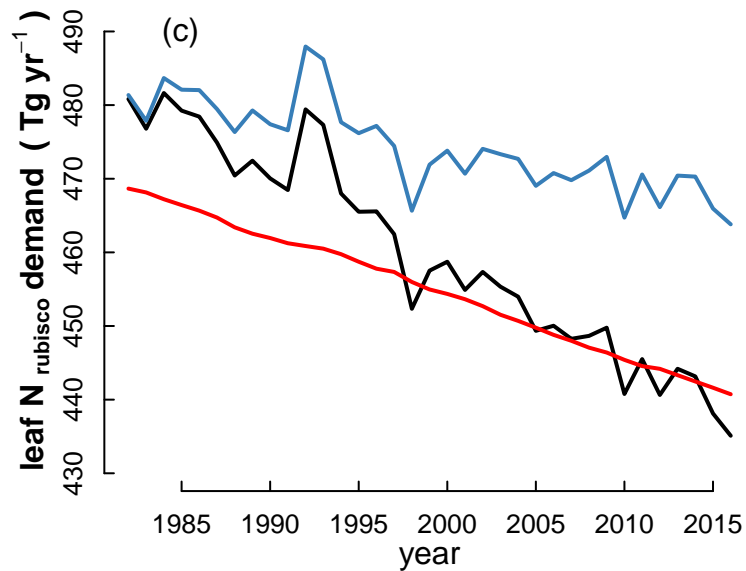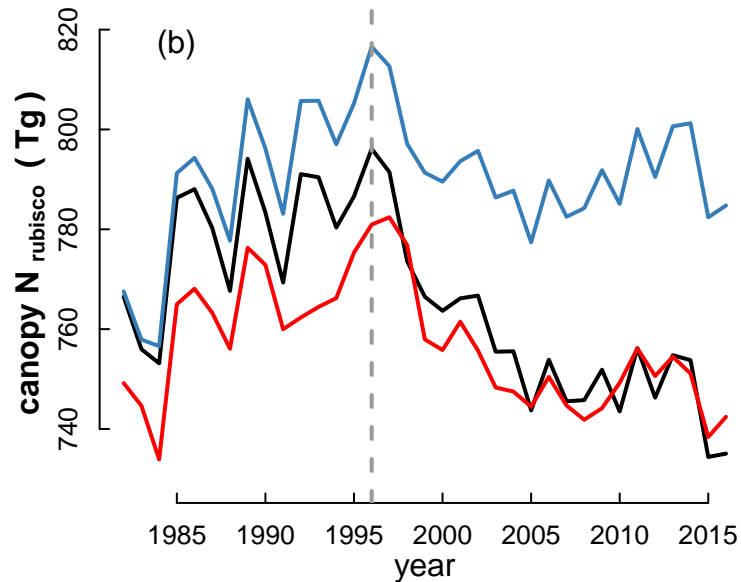
(a)

(b)

(c)

$V_{cmax,chl}$ (μmol m^{-2}s^{-1})

(a)

V_{cmax} (μmol m^{-2}s^{-1})

(b)

V_{cmax} (μmol m^{-2}s^{-1}yr^{-1}) $V_{cmax,25}$ (μmol m^{-2}s^{-1}yr^{-1})

(a)   (b)

only climate V_{cmax} (μmol m^{-2}s^{-1}yr^{-1})   only climate $V_{cmax,25}$ (μmol m^{-2}s^{-1}yr^{-1})

(c)   (d)

only CO$_2$ V_{cmax} (μmol m^{-2}s^{-1}yr^{-1})   only CO$_2$ $V_{cmax,25}$ (μmol m^{-2}s^{-1}yr^{-1})
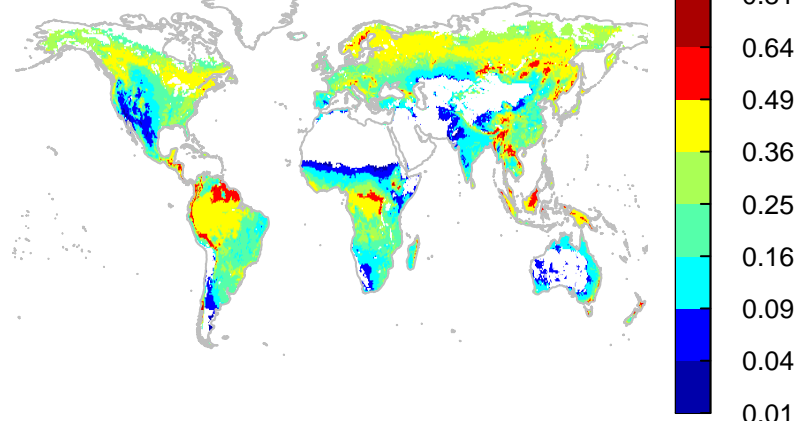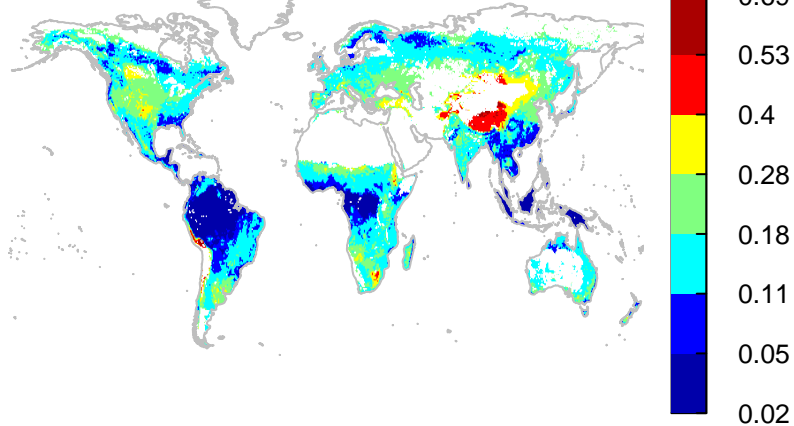
(e)   (f)
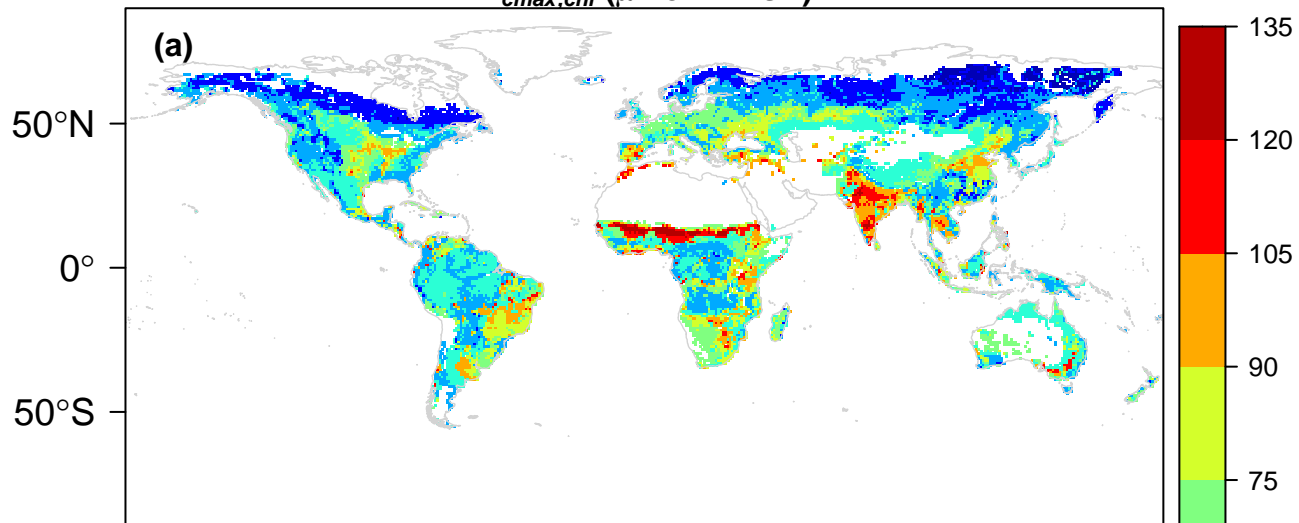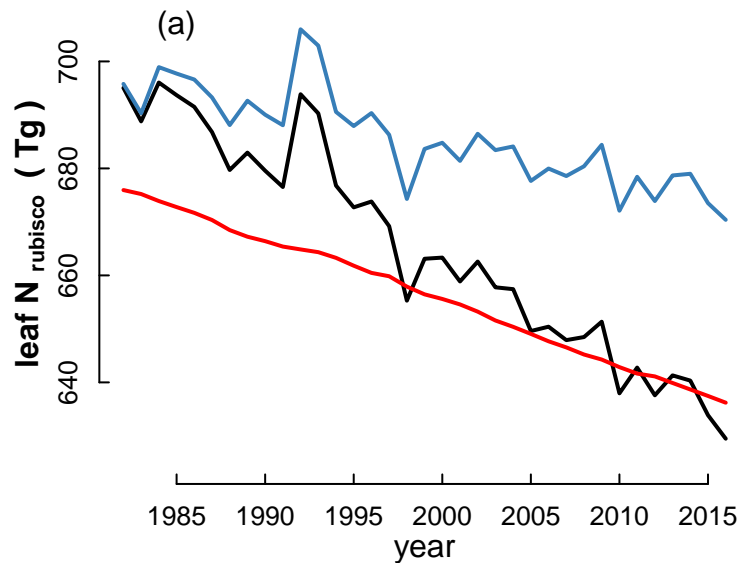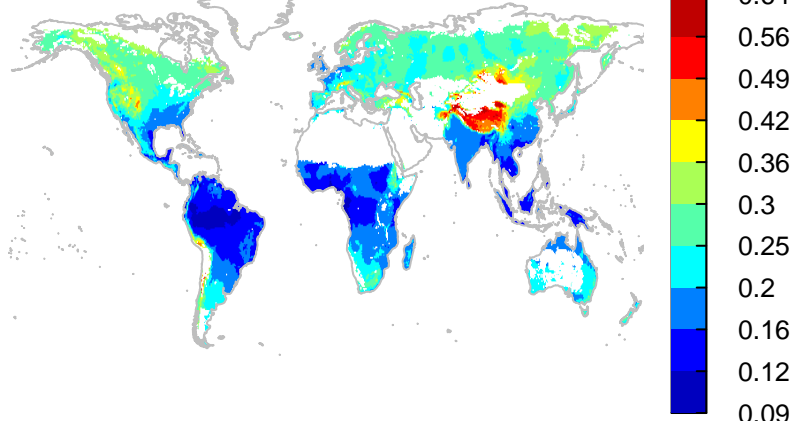
(a) leaf $N_{rubisco}$ (g m^{-2})

(b) canopy $N_{rubisco}$ (g m^{-2})

(c) leaf $N_{rubisco}$ demand (g m^{-2} yr^{-1})

(d) canopy $N_{rubisco}$ demand (g m^{-2} yr^{-1})